Taylor & Francis
Taylor & Francis Group

Canadian Metallurgical Quarterly

The Canadian Journal of Metallurgy and Materials Science

ISSN: 0008-4433 (Print) 1879-1395 (Online) Journal homepage: www.tandfonline.com/journals/ycmq20

Optimisation of iron ore flotation parameters using response surface methodology

Tarcísio Gonçalves de Brito, Tiago Caixeta Nunes, Wender Roger Ramos, Emerson José de Paiva, Carlos Henrique de Oliveira, Ricardo Luiz Perez Teixeira, José Carlos de Lacerda & Rogério Fernandes Brito

To cite this article: Tarcísio Gonçalves de Brito, Tiago Caixeta Nunes, Wender Roger Ramos, Emerson José de Paiva, Carlos Henrique de Oliveira, Ricardo Luiz Perez Teixeira, José Carlos de Lacerda & Rogério Fernandes Brito (18 May 2026): Optimisation of iron ore flotation parameters using response surface methodology, Canadian Metallurgical Quarterly, DOI: 10.1080/00084433.2026.2668302

To link to this article: https://doi.org/10.1080/00084433.2026.2668302

Published online: 18 May 2026.

CANADIAN METALLURGICAL QUARTERLY
https://doi.org/10.1080/00084433.2026.2668302

Optimisation of iron ore flotation parameters using response surface methodology

Tarcísio Gonçalves de Brito [a], Tiago Caixeta Nunes[b], Wender Roger Ramos[a], Emerson José de Paiva[a], Carlos Henrique de Oliveira[a], Ricardo Luiz Perez Teixeira[a], José Carlos de Lacerda[a] and Rogério Fernandes Brito[a]

[a]Institute of Integrated Engineering, Federal University of Itajubá, Itabira, Brazil; [b]Vale SA, Iron Ore Beneficiation Process Control and Optimization, Itabira, Brazil

ABSTRACT

This study investigates the optimisation of process parameters in the reverse cationic flotation of iron ore using Response Surface Methodology (RSM) and the Generalised Reduced Gradient (GRG) algorithm. A Central Composite Design (CCD) was used to evaluate the effects of starch dosage, amine collector dosage, and pH on metallic recovery (R_m) and SiO_2 content in the concentrate. The results indicated that starch and amine dosages significantly influence recovery, while the SiO_2 response model, despite its lower statistical significance ($p = 0.310$), provided a reliable trend for constrained optimisation. The optimal conditions were identified as 500 *g/t* of starch, 75 *g/t* of amine, and pH 9.80. Experimental validation of these parameters yielded a metallic recovery of 93.86% and a SiO_2 content of 0.51%, demonstrating strong agreement with model predictions (1 < 1.35% deviation). The integration of RSM and GRG proved to be an effective approach for balancing high metallurgical recovery with strict concentrate quality specifications, providing a robust tool for decision-making in iron ore beneficiation.

Cette étude examine l'optimisation des paramètres du procédé de flottation cationique inverse du minerai de fer en utilisant la méthodologie des surfaces de réponse (RSM) et l'algorithme de gradient réduit généralisé (GRG). On a utilisé un plan composite centré (CCD) pour évaluer les effets du dosage d'amidon, du dosage de collecteur aminé et du pH sur la récupération métallique (R_m) et la teneur en SiO_2 dans le concentré. Les résultats ont indiqué que les dosages d'amidon et d'amine influençaient significativement la récupération, tandis que le modèle de réponse du SiO_2, malgré sa plus faible signification statistique (p = 0.310), a fourni une tendance fiable pour l'optimisation sous contraintes. On a identifié les conditions optimales à 500 *g/t* d'amidon, 75 *g/t* d'amine et un pH de 9.80. La validation expérimentale de ces paramètres a produit une récupération métallique de 93.86% et une teneur en SiO_2 de 0.51%, démontrant une forte concordance avec les prédictions du modèle (écart <1.35%). L'intégration des méthodes RSM et de GRG s'est montrée une approche efficace pour équilibrer une récupération métallurgique élevée et des spécifications strictes en matière de qualité du concentré, offrant un outil robuste pour la prise de décision dans le traitement du minerai de fer.

ARTICLE HISTORY
Received 22 January 2026
Accepted 24 April 2026

KEYWORDS
Iron ore flotation; reverse cationic flotation; response surface methodology; optimisation; GRG algorithm; metal recovery; mineral processing

1. Introduction

Flotation is a physicochemical concentration process that exploits differences in the surface properties of the minerals present in a pulp. This process is primarily carried out in mechanical flotation cells, which consist of a tank equipped with an agitation system, pulp level control, aeration, and froth collection mechanisms [1]. According to [2], flotation is the most widely applied method for the concentration of iron ores with particle sizes of less than 0.150 mm. By inducing the hydrophobicity of mineral particles through the selective adsorption of cationic collectors, it is possible to achieve an effective separation of quartz (SiO_2), the main gangue mineral associated with iron ores, by distinguishing hydrophobic particles (air-affine) from hydrophilic ones (water-affine) such as starch-depressed iron oxides [3].

The quality of the concentrate obtained through flotation is determined by established specifications and is influenced by several operational variables, including pH, starch depressant dosage, amine collector dosage, particle size distribution, and rotor speed [4]. In reverse flotation, the SiO_2 content in the concentrate is the primary quality indicator for direct reduction pellet feed. This study examines the reverse cationic flotation process employed in iron ore beneficiation. Among available technologies, flotation stands out as the most

CONTACT Tarcísio Gonçalves de Brito tgbrito@unifei.edu.br Institute of Integrated Engineering, Federal University of Itajubá, Itabira, Brazil

efficient method, both technically and economically, for producing high-grade iron concentrates [3,5]. Two key indicators are typically employed to evaluate the efficiency of the cationic quartz flotation process: metal recovery (R_m) and the SiO_2 content in the concentrate. While SiO_2 content is directly determined through chemical analysis of laboratory samples, R_m is a derived parameter that depends on the iron content of the feed, concentrate, and tailings streams [6]. These measurements are essential for assessing the influence of process control variables such as starch concentration, amine dosage, and pH on flotation performance and for guiding process optimisation [7].

Numerous studies have applied statistical methodologies, such as Response Surface Methodology (RSM), to investigate the effects of these variables on iron recovery and SiO_2 content [8–10]. The application of such methods facilitates the identification of statistically significant models, which help minimise process variability and ensure conformity with product specifications, such as the strict limit of $SiO_2 \leq 0.50\%$ [11]. In this context, the present study aims to enhance the flotation process by applying a methodological framework to maximise R_m while maintaining the SiO_2 content below the upper specification limit. The proposed approach employs design of experiments (DoE), statistical modelling, and the Generalised Reduced Gradient (GRG) optimisation algorithm to determine the optimal combination of process parameters. The iron ore sample investigated was obtained from a mining complex located in the Iron Quadrangle region of Minas Gerais, Brazil. In this beneficiation plant, approximately 67% of production corresponds to pellet feed derived from a flotation circuit composed of conventional self-aerated flotation cells. The concentrate obtained from the recleaner stage, also referred to as the final flotation product, contains approximately 68.0% Fe, with an average metal recovery of around 89.0%.

2. Statistical tools and optimization algorithm

Statistical modelling techniques are employed to establish quantitative relationships between process inputs and outputs, resulting in predictive models that guide industrial decision-making [2,12]. In this study, Response Surface Methodology (RSM) was utilised to map the experimental domain and identify optimal operating conditions. The experimental design followed a Central Composite Design (CCD), which is particularly effective for capturing second-order effects and curvature in flotation processes. The statistical significance of the generated models was assessed via Analysis of Variance (ANOVA), using parameters such as the p-value, coefficient of determination (R^2), and lack-of-fit tests to ensure predictive reliability. To solve the resulting multi-objective optimisation problem, maximising R_m while constrained by $SiO_2 \leq 0.50\%$, the Generalised Reduced Gradient (GRG) nonlinear algorithm was implemented. The GRG method is robust for handling smooth nonlinear constraints, allowing for the identification of optimal factor levels (starch, amine, and pH) that satisfy strict industrial quality specifications while minimising operational variability and costs [13].

2.1. Response surface methodology (RSM)

Response Surface Methodology (RSM) was employed in this study as part of the Design of Experiments (DoE) framework. RSM encompasses a suite of mathematical and statistical techniques for analysing and modelling processes in which a response variable is influenced by multiple independent factors [11]. This methodology is widely applied in mineral processing to optimise complex operations where variables interact non-linearly [14,15]. RSM utilises second-order polynomial formulations, incorporating hypothesis testing, Analysis of Variance (ANOVA), and regression analysis to construct predictive models. The identification of stationary points, whether a maximum, minimum, or saddle point, is achieved through the computation of gradients and Hessians of the derived functions [9,15]. To accurately capture the curvature of the response surface in the flotation process, a quadratic model is required, as represented by Equation (1):

$$Y = \beta_0 + \sum_{i=1}^{k} \beta_i x_i + \sum_{i=1}^{k} \beta_{ii} x_i^2 + \sum_{i<j} \sum \beta_{ij} x_i x_j + \varepsilon \quad (1)$$

where y is the response of interest, β_0 is a constant, β_i are the linear coefficients, β_{ii} are the quadratic coefficients, β_{ij} are the interaction coefficients, and ε is the experimental error. According to [11], the β parameters of the model can be estimated using the Ordinary Least Squares (OLS) method. The OLS estimator minimises the sum of squared residuals and can be represented in matrix form by Equation (2):

$$\hat{\beta} = (X^T X)^{-1} X^T Y \quad (2)$$

where β is the polynomial coefficient, X is the matrix of coded factors, and Y is the response of interest.

To conduct experiments efficiently, the chosen factors and their levels must be varied systematically to identify influential parameters while accounting for

experimental variability. Among the available experimental designs, the Central Composite Design (CCD) stands out for its ability to model second-order response surface functions with a reduced number of runs [15,16]. A CCD is structured around three distinct sets of experimental points: (i) a full factorial design (2^k) or a fractional factorial design (2^{k-p}), where p denotes the degree of fractionation; (ii) a set of centre points used to estimate experimental error and curvature; and (iii) a group of axial points α that represent extreme levels. When the distance from the design centre to the factorial points is normalised to unity, the distance to each axial point is denoted by α. This parameter α is critical for conferring rotatability to the design, ensuring that the variance of the predicted response is constant for all points equidistant from the centre. The total number of experimental runs (N) required for a CCD is determined by Equation (3):

$$N = 2^k + 2k + n_c \tag{3}$$

where N represents the total number of experimental runs, k denotes the number of factors or input variables, 2^k corresponds to the number of factorial points, $2k$ indicates the number of axial points, and n_c refers to the number of centre points included in the design.

The significance of each factor and its interactions is assessed through the p-value, representing the probability of observing the effect by chance under the null hypothesis. In this study, a significance level of $\alpha = 0.05$ was adopted; thus, factors with p-values less than 0.05 were considered statistically significant [11]. The adequacy of the fitted model is expressed through the coefficient of determination (R^2), which quantifies the proportion of response variance explained by the model [17,18]. Complementarily, the adjusted coefficient of determination (R^2_{adj}) was utilised, as it accounts for the number of predictors in the model, providing a more reliable estimate of the model's explanatory power by correcting for the degrees of freedom [19].

2.2. Generalised reduced gradient algorithm

According to [19], a multiple-response problem is typically formulated as a constrained optimisation problem. In this study, one response variable is designated as the primary objective, while the remaining responses are treated as operational constraints. The Generalised Reduced Gradient (GRG) algorithm is widely recognised for its robustness and computational efficiency in solving such nonlinear optimisation problems. As noted by Köksoy [20], GRG is classified as a primal or feasible-direction method, identifying optimal solutions by conducting searches within feasible regions [21]. A significant advantage of this method is that it does not strictly depend on structural properties such as convexity in the solution space. Furthermore, the GRG algorithm exhibits satisfactory global convergence, particularly when initialised in proximity to the expected optimal zone [22]. The term 'reduced gradient' refers to the technique of substituting constraints into the objective function, thereby reducing the problem's dimensionality and the number of gradients to be computed [13,19]. According to [22], a general representation of a nonlinear programming problem solved by GRG can be expressed as shown in Equation (4):

$$\begin{aligned} &\text{Minimize} && f(x) \\ &\text{Subject to:} && g_i(x) = 0,\ i = 1,\ \ldots,\ m \\ &&& l_j \le x_j \le u_j,\ j = 1,\ \ldots,\ n \end{aligned} \tag{4}$$

Where f represents the objective function, g denotes the constraints, and x is a vector of n process variables ($x_1, x_2, \ldots, x_n$) bounded by lower limits l_j and upper limits u_j. To handle inequality constraints (such as $SiO_2 \le 0.50\%$), the algorithm converts them into equality constraints by introducing slack variables. The general GRG model transforms the constrained optimisation problem into an unconstrained one by directly substituting the constraints. As described by Chen and Fan [12], Lasdon et al. [22], the vector of process variables x is partitioned into two subvectors: independent variables (x_i) and dependent (or basic) variables (x_d). This partitioning allows the nonlinear programming (NLP) problem to be reformulated in a reduced form, as illustrated in Equation (5):

$$\nabla_r f = \frac{\partial f}{\partial x_i} - \frac{\partial f}{\partial x_d}\left(\frac{\partial g}{\partial x_d}\right)^{-1}\frac{\partial g}{\partial x_i} \tag{5}$$

The term $\nabla_r f$ the reduced gradient, which guides the search for the optimal solution within the feasible region defined by the operational constraints of the flotation process [13]. The GRG algorithm determines a search direction for optimising the objective function by starting from an initial feasible point, $x(0)$. This search direction is derived from the reduced gradient (g), as expressed in Equation (6).

$$r^k(x_N) = \left[\frac{\partial f^k}{\partial x_N^k}\right]^T - \left[\frac{\partial f^k}{\partial x_B^k}\right]^T \left[\frac{\partial g^k}{\partial x_B^k}\right]^{-1} \left[\frac{\partial g^k}{\partial x_N^k}\right] \tag{6}$$

The iterative search for the algorithm's optimal solution terminates when the magnitude of the reduced gradient falls below a predefined tolerance threshold. If this condition is not met, the algorithm identifies a new point along the search direction defined by the reduced gradient. This process is repeated until the best feasible

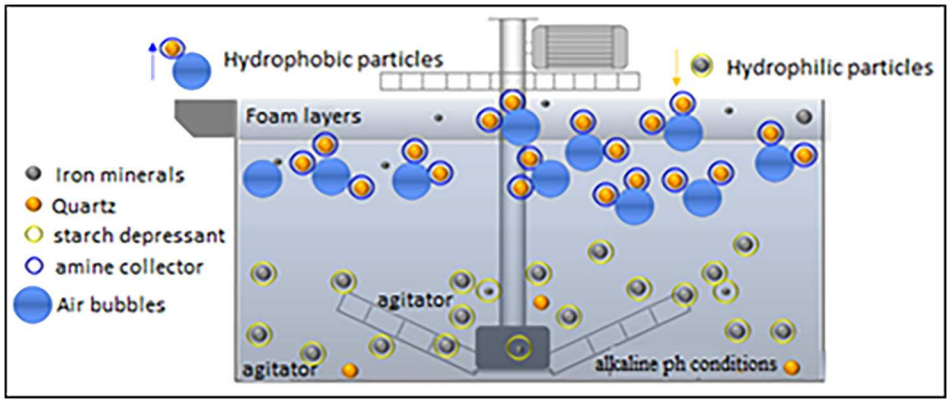

Figure 1. Bubble-particle adhesion phenomenon in quartz flotation.

solution (the local or global optimum) is obtained within the specified constraints [22].

3. Iron ore concentration by flotation

The selection of the most suitable method for iron ore concentration requires a comprehensive evaluation of the mineralogical characteristics of both iron-bearing and gangue minerals [23]. Iron oxide concentration, particularly in ores with significant silica (SiO_2), is primarily achieved through the flotation of quartz [5,10]. Mineralogical analysis of the sample investigated indicates that the flotation feed comprises approximately 66.21% iron oxide and 33.16% quartz. Flotation is a physicochemical process that exploits differences in surface properties, involving heterogeneous particles suspended in an aqueous pulp with the introduction of a gaseous phase [5]. This process is vital due to the depletion of high-grade deposits and the demand for concentrates with high iron (Fe) content and minimal impurities (SiO_2, Al_2O_3, and phosphorus) [2]. The present study focuses on reverse cationic flotation of quartz, the most common method in Brazil for particles below 0.150 mm. In the investigated plant, 75% of this fraction is naturally liberated from hydrocyclones and high-frequency sieves, while 25% comes from the grinding circuit. The particle size distribution must comply with pelletising standards to produce 'pellet feed'. During flotation, quartz particles are rendered hydrophobic by cationic amine under alkaline conditions and recovered in the froth (tailings). Simultaneously, iron oxides are kept hydrophilic through the addition of starch as a depressant, remaining in the pulp phase to enhance metal recovery (R_m) [24]. This process is illustrated schematically in Figure 1.

When assessing the efficiency of reverse cationic flotation for iron ore, both the SiO_2 content in the concentrate and the metal recovery (R_m) were evaluated. The quality of the concentrate is directly associated with the controlled and optimised dosages of the reagents. Three primary process control parameters are manipulated: starch (depressant), cationic etheramine (collector), and pH (surface charge modifier) [7]. Understanding the surface properties of the mineral species is essential, as they govern the adsorption dynamics and selectivity of the reagents. Variations in mineral surfaces result in differing degrees of hydrophobicity, which dictate the interaction between particles and air bubbles. Furthermore, flotation efficiency is known to decrease when the particle size exceeds the limit that can be effectively carried by the bubbles, a factor that underscores the importance of the 0.150 mm liberation size mentioned previously [25].

4. Materials and methods

4.1. Ore preparation, reagents, and equipment

The material investigated in this study consists of iron ore samples collected from the global fraction below 0.150 mm, obtained from 22 drill holes across nine regions within the mining area (spaced ~1.5 km apart). To ensure a representative composite sample for bench-scale flotation, the preparation reflected the chemical, physical, and mineralogical variations expected in a future Run-of-Mine (ROM) scenario, accounting for the inherent heterogeneity of the mining fronts.

The reagents employed were:

Collector: A commercial cationic ether-amine prepared at a mass concentration of 2%. The amine was neutralised to 50% using acetic acid to ensure adequate solubility and collector efficiency.

Depressant: Corn grits (starch) prepared via caustic gelatinisation at a mass concentration of 1%. The depressant-to-NaOH mass ratio was maintained at 5:1

Table 1. Levels and control parameters for the experiment.

			Levels				
Control variables	Symbols	Unit	$-\alpha$	−1	0	1	α
Starch	(A_{md})	g/t	299	350	425	500	551
Amine	(A_{mn})	g/t	32	75	138	200	243
Flotation	pH	–	9.60	9.80	10.15	10.50	10.70

to ensure complete starch degradation and high selectivity for iron oxides.

pH Modifier: Sodium hydroxide (NaOH) solutions were used to achieve the target alkalinity levels defined by the experimental design.

Chemical analyses were performed using X-ray Standard XRF spectrometer. Particle size distribution for fractions above 0.045 mm was determined using Tyler series sieves, while the sub-0.045 mm fraction was measured using a Cilas 1064 granulometer. Mineralogical characterisation was performed via reflected light optical microscopy to quantify mineral phases and evaluate the degree of liberation between iron oxides and quartz (SiO_2).

4.2. Experimental procedure

The experimental design incorporated three control variables: starch depressant dosage (A_{md}), amine collector dosage (A_{mn}), and flotation pH. The levels for these parameters, including the centre points, were established based on a 12-month operational history preceding the study. This approach ensured that the experimental range was representative of potential future operating conditions. The control variables and their respective coded and real levels are summarised in Table 1. It is important to note that the pH was adjusted using NaOH solutions to reach the specific target values of the experimental matrix before each flotation test, ensuring that the chemical interactions occurred at the intended alkalinity level. Flotation tests were performed in a bench-scale sub-aeration cell (Model CDC, 1.5 L), rotor speed (900 rpm) and analytical equipment (Cilas 1064, XRF spectrometer) has been added to Sections 4.1 and 4.2 and an air flow rate of L/min. Conditioning was carried out at 50% solids by weight to ensure high energy dissipation and efficient reagent-mineral surface contact, a common practice in Brazilian iron ore beneficiation to optimise starch and amine adsorption. Subsequent flotation was conducted by adjusting the pulp to the cell's working volume.

In this study, the statistical software Minitab® 17 was employed to generate the experimental matrix based on a Central Composite Design (CCD). The design comprised 17 flotation experiments organised into three distinct groups: a full factorial design $2^k = 8$ experiments), an axial point set ($2k = 6$ experiments), and a centre point set (3 replicates). The axial distance (α), representing the radius of the experimental region to ensure rotatability, was calculated as $\alpha = (2^k)^4 = 1.682$. The complete experimental matrix, including the randomised order of the runs to minimise systematic errors, is presented in Table 2.

The flotation experiments were conducted using a Dharma mechanical flotation cell with a 2600 mL tank, encompassing two stages: rougher/cleaner and scavenger. The ore was mixed with fresh water to

Table 2. Experimental matrix – central composite design.

	Parameters		
Test no.	Starch (A_{md}, g/t)	Amine (A_{mn}, g/t)	pH
1	350	75	9.80
2	500	75	9.80
3	350	200	9.80
4	500	200	9.80
5	350	75	10.50
6	500	75	10.50
7	350	200	10.50
8	500	200	10.50
9	299	137.5	10.15
10	551	137.5	10.15
11	425	32	10.15
12	425	243	10.15
13	425	137.5	9.56
14	425	137.5	10.74
15	425	137.5	10.15
16	425	137.5	10.15
17	425	137.5	10.15

Table 3. Particle size distribution of the delaminated sample.

	Particle size distribution (%)		
Size fraction (mm)	Retained mass (%)	Cumulative passing (%)	Cumulative passing
0.210	0.00	0.00	100.00
0.150	0.25	0.25	99.75
0.106	12.67	12.92	87.08
0.075	23.92	36.83	63.17
0.045	29.58	66.42	33.58
0.037	8.94	75.35	24.65
0.025	14.09	89.44	10.56
0.015	7.94	97.38	2.62
0.010	1.52	98.90	1.10
0.006	0.66	99.56	0.44
0.005	0.16	99.73	0.27
0.004	0.15	99.88	0.12
0.0032	0.10	99.98	0.02
−0.0032	0.02	100.00	0.00
Total	100.00	–	–

Table 4. Distribution of the main chemical elements of the global samples that form the flotation feed, which had a loss on ignition of 0.38.

Fe	SiO_2	*P*	Al_2O_3	Mn	TiO_2	CaO	MgO	LOI
49.24	28.36	0.016	0.33	0.022	0.039	0.008	0.001	0.38

achieve a solids concentration of 50% (by weight) and conditioned for 3 min. While industrial process water typically recirculates with ~4% solids, fresh water was used here to ensure experimental control. For each run, the pulp pH was initially monitored and then precisely adjusted using NaOH to match the specific target levels defined in the experimental matrix (Table 2). This adjustment occurred after the mineral was pulped but prior to the addition of collectors and air intake. Following pH stabilisation, the reagents were added: starch was conditioned for 3 min, followed by amine for 1 min. All experiments were performed at a rotor speed of 1200 RPM. The scavenger stage used the tailings from the preceding rougher/cleaner stage as feed material. In both stages, flotation was conducted to exhaustion meaning froth collection continued until no further mass recovery was observed. This 'flotation to limit' approach was specifically designed to evaluate the minimum achievable SiO_2 content in the final concentrate under the optimised chemical conditions [25].

5. Results and discussion

Based on the flotation test results organised according to the CCD framework, this study demonstrates the applicability of the proposed methodological approach for iron ore concentration. Mathematical modelling and Analysis of Variance (ANOVA) were performed to evaluate the significance of the main effects and their interactions. Subsequently, the GRG algorithm was applied to identify the optimal parameter conditions for maximising metal recovery (R_m) while strictly maintaining the SiO_2 content in the concentrate below the industrial limit of 0.50%. Finally, confirmatory flotation tests were conducted under these optimised conditions to validate the predictive capability of the models and ensure the reliability of the proposed optimisation.

5.1. Sample characterization

The results of the particle size distribution analysis indicate that 66.2% of the total mass is concentrated between the −0.150 mm and +0.045 mm fractions. The highest proportion of the sample (29.6%) corresponds to the +0.045 mm fraction, while no coarse material was detected above 0.210 mm. The fine fraction passing through the 0.045 mm sieve represents 33.6% of the sample, with a minor portion (1.1%) consisting of ultrafine particles (−0.010 mm). The complete granulometric profile is presented in Table 3. This specific size range is ideal for reverse cationic flotation, as it ensures a high degree of mineral liberation while remaining within the hydraulic transport limits of the air bubbles in the flotation cell [25].

As presented in Table 4, the chemical analysis of the flotation feed revealed low concentrations of contaminants such as Al_2O_3, phosphorus (P), and manganese (Mn). The Loss on Ignition (LOI), representing the volatile constituents, also remained at minimal levels. These results confirm that the ore is primarily composed of iron oxides and quartz, justifying the focus of this study on the selective separation of SiO_2.

Mineralogical quantification via light microscopy revealed a predominant composition of free hematite and quartz, with an exceptionally high total liberation degree of 98.23%. The principal mineral phases are illustrated in the photomicrographs in Figure 2. Under reflected light, quartz is identified by its dark grey colouration and morphological variations. The quartz grains typically exhibit well-defined edges, appearing compact and mostly free of associations, with only rare occurrences of binary particles linked to compact hematite grains. This high degree of liberation is a critical factor that favours the high selectivity observed during the reverse cationic flotation process.

5.2. Modelling the responses

The experimental results for all 17 runs are summarised in Table 5. Analysis of the data reveals that the SiO_2 content in the concentrate remained below 1.00% in nearly all trials, with the exception of a single outlier in experiment 11. To meet strict industrial standards, a maximum limit of 0.50% SiO_2 combined with maximised metal recovery (R_m) was established as the primary optimisation criterion. Remarkably, 11 out of the 17 experiments successfully achieved SiO_2 levels below 0.50%, while three experiments surpassed the average metal recovery of 89.0%. Among the tested conditions, experiment 2 exhibited the most superior performance, yielding a high-quality concentrate with only 0.43%

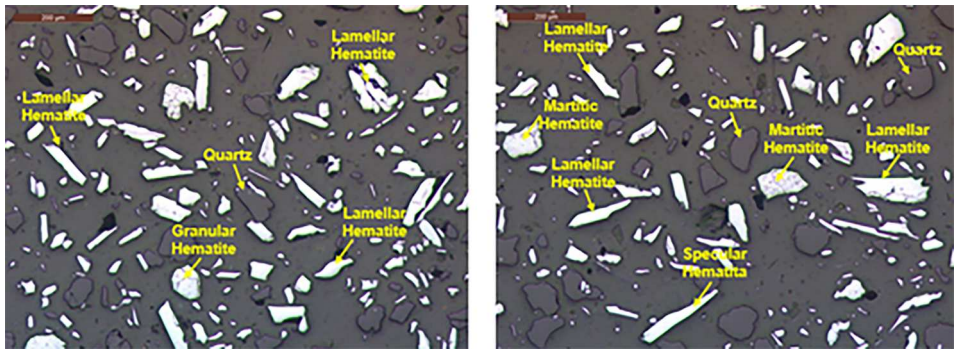

Figure 2. Photomicrographs of the main minerals found in the sample.

SiO_2 and a substantial metal recovery (R_m) of 93.50%. These preliminary findings suggest a robust correlation between the reagent dosages and the flotation efficiency, which will be further quantified through statistical modelling.

The adequacy of the regression models was evaluated using Analysis of Variance (ANOVA), as summarised in Table 6. The model for metallic recovery (R_m) demonstrated exceptional statistical significance ($p < 0.001$) and a high adjusted coefficient of determination ($R^2adj =$ 94.78%). Furthermore, the non-significant lack-of-fit ($p = 0.094$) confirms that the model is highly reliable for predicting recovery within the experimental range. Regarding the SiO_2 content, the model did not achieve conventional statistical significance ($p = 0.310$ $), and a marginal lack-of-fit ($p = 0.046$) was observed. This is primarily attributed to the high consistency of the results, as most experiments achieved silica levels below 0.60%, with the notable exception of the outlier in experiment 11 (10.68%). While the SiO_2 model is less robust for precise mathematical prediction, it remains a valid indicator of the process limits, showing that the established reagent dosages are sufficient to keep silica within industrial specifications in 16 out of 17 conditions.

Both response variables exhibited p-values greater than the 0.05 significance threshold in the normality test: 0.069 for the SiO_2 content and 0.153 for metallic recovery (R_m). This indicates that the data sets follow a normal distribution, validating the reliability of the experimental results. Overall, the responses were satisfactory, although the lack of statistical significance and the relatively low fit of the SiO_2 model are attributed to the inherent mineralogical heterogeneity of the material. This variability arises from the composite nature of the sample, which consists of aliquots from 22 drill hole samples collected across nine distinct regions of the mining area. Such a wide-ranging composite represents the real industrial feed more accurately than a homogenised laboratory sample, justifying the marginal adjustments in the silica model.

The regression equations of the full quadratic models for the respective responses are presented in Equations

Table 5. Responses of flotation tests.

	Coded parameters			Current parameters			Responses	
N test	x_1	x_2	x_3	Starch (A_{md}, g/t)	Amine (A_{mn}, g/t)	pH	SiO_2%	R_m%
1	−1	−1	−1	350	75	9.80	0.65	90.02
2	1	−1	−1	500	75	9.80	0.43	93.50
3	−1	1	−1	350	200	9.80	0.37	79.75
4	1	1	−1	500	200	9.80	0.37	86.39
5	−1	−1	1	350	75	10.50	0.51	90.70
6	1	−1	1	500	75	10.50	0.56	95.11
7	−1	1	1	350	200	10.50	0.46	79.88
8	1	1	1	500	200	10.50	0.44	89.59
9	$-\alpha^{(1)}$	0	0	299	138	10.15	0.48	80.01
10	A	0	0	551	138	10.15	0.74	92.19
11	0	$-\alpha$	0	425	32	10.15	**10.68**	98.03
12	0	α	0	425	243	10.15	0.68	85.98
13	0	0	$-\alpha$	425	138	9.60	0.32	88.25
14	0	0	α	425	138	10.70	0.36	89.45
15	0	0	0	425	138	10.15	0.35	87.59
16	0	0	0	425	138	10.15	0.31	87.13
17	0	0	0	425	138	10.15	0.37	87.93

(1) - The value of $\alpha = 1.68$.

Table 6. Analysis of variance (ANOVA) for the flotation response models (R_m and SiO_2).

Response	DF	Adj. SS	Adj. MS	*F*-value	*P*-value	Lack-of-fit	*S*	R^2 (%)	R^2 (*adj.*) (%)
SiO_2(%)	9	0.185094	0.20566	1.53	0.310	0.046	0.115763	69.72	24.29
R_m(%)	9	312.047	34.672	31.27	0.000	0.094	1.052950	97.91	94.78

(7) and (8).

$$\begin{aligned} SiO_2\% = &- 8.1 - 0.0236Amd - 0.0198Amn \\ &+ 2.89\text{pH} + 0.000013Amd^2 \\ &+ 0.000027Amn^2 - 0.171\text{pH}^2 \\ &+ 0.000004Amd \cdot Amn + 0.00119Amd \cdot \text{pH} \\ &+ 0.00097Amn \cdot \text{pH} \end{aligned} \tag{7}$$

$$\begin{aligned} R_m\% = &\ 349 - 0.070Amd - 0.317Amn - 46.9\text{pH} \\ &- 0.000130Amd^2 + 0.000357Amn^2 \\ &+ 1.95\text{pH}^2 + 0.000225Amd \cdot Amn \\ &+ 0.0190Amd \cdot \text{pH} \\ &+ 0.0059Amn \cdot \text{pH} \end{aligned} \tag{8}$$

While Equations (7) and (8) are presented in real units for practical application, their respective coded versions were used to confirm that amine dosage is the most significant factor influencing both responses.

5.3. Analysis of the parameters main effects

To isolate the impact of each independent variable on the process responses, parameters were varied individually while maintaining the remaining factors at their respective central points. The relationship between each parameter and the response may exhibit a linear trend, indicating the dominance of the main term, or a parabolic curvature, indicating a significant quadratic effect. The individual effects of each parameter on the SiO_2 content in the concentrate are illustrated in Figure 3. All three parameters displayed distinct curvature patterns. For starch dosage (A_{md}), the minimum SiO_2 content was achieved at approximately 420 *g*/*t*. For the amine collector (A_{mn}), the lowest SiO_2 levels occurred near 150 *g*/*t*. Conversely, pH exhibited minor variations, with a fluctuation of only 0.30% in SiO_2 content and a slight maximum around pH 10.25. A critical observation was that reducing the amine dosage below 70 *g*/*t* led to a pronounced increase in SiO_2 content, as the collector concentration became insufficient for quartz flotation. Furthermore, SiO_2 levels exceeding the 0.50% specification limit were observed at both high amine dosages and extreme starch concentrations (both low and high). Considering the quadratic effects, amine dosage demonstrated the greatest statistical significance compared to starch dosage and pH, confirming its role as the primary driver for silica removal in this cationic reverse flotation system.

As observed in Figure 3, the parabolic nature of the curves for starch and amine indicates that there is an optimal dosage range for silica depression and collection, respectively. The sharp rise in SiO_2 at lower amine levels (left side of the amine plot) highlights the critical threshold for collector effectiveness. Conversely, the flatter profile of the pH plot suggests that, within the tested range of 9.5–11.0, pH has a secondary influence compared to the reagent dosages. As illustrated in Figure 4, the amine dosage exhibited the most pronounced influence on metal recovery (R_m). An increase in amine dosage led to a continuous reduction in R_m, indicating an inverse relationship between these variables due to the potential flotation of iron oxides at higher collector concentrations.

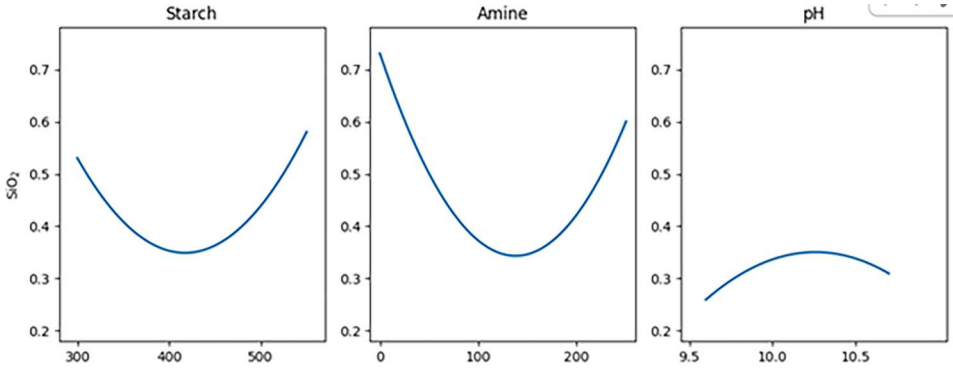

Figure 3. Main effects of starch, amine, and pH on SiO2 content. Note: While one factor is varied, others are held constant at their central points (Starch: 400 *g*/*t*, Amine: 100 *g*/*t*, pH: 10.0).

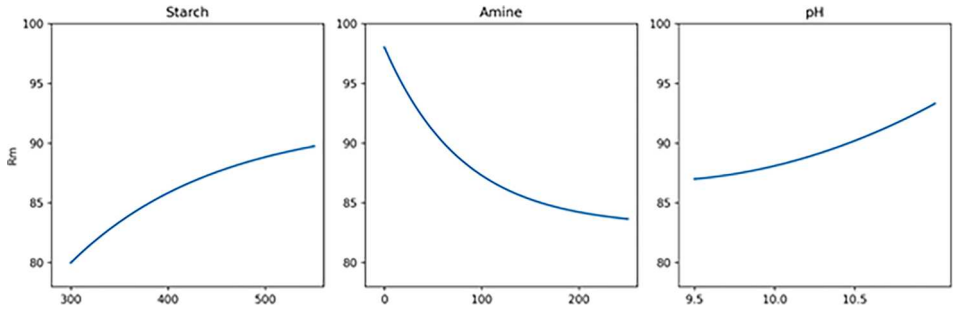

Figure 4. Main effects on the metallic recovery (R_m).

Conversely, increasing the starch dosage resulted in higher metal recovery, demonstrating a positive correlation as the depressant effectively inhibits hematite flotation. Regarding pH, a slight increase in R_m was observed with rising pH values, although this effect was comparatively less significant than the reagent dosages.

The behaviour observed in Figure 4 highlights the high sensitivity of the process to the amine dosage. The steep negative slope indicates that excessive collector concentration promotes the flotation of iron-bearing minerals, significantly reducing R_m. In contrast, the positive slope for starch dosage confirms its efficacy as a selective depressant for hematite. The relatively flat profile for pH suggests a robust operational window between 9.5 and 11.0, where recovery remains largely stable.

5.4. Analysis of parameter interaction effects

The interaction effects on the SiO_2 content in the concentrate are illustrated through the response surfaces and contour plots in Figure 5. The interaction between starch and amine (Figure 5(a)) reveals a well-defined elliptical region where silica levels reach their minimum (below 0.30%). This 'valley' indicates that an optimal balance between quartz collection and iron oxide depression is achieved near the central experimental points (approximately 420 g/t of starch and 150 g/t of amine). Deviations from this region, particularly towards high starch and high amine dosages, lead to a significant increase in silica, likely due to competitive adsorption at the mineral surfaces. In contrast, the interactions involving pH (Figure 5(b,c)) exhibit a characteristic saddle-shaped profile. This topology demonstrates that the process is remarkably robust regarding pH fluctuations between 9.5 and 10.5. The broad blue zones in the contour plots indicate that industrial specifications ($SiO_2 < 0.50\%$) are consistently met across a wide range of reagent combinations. However, the upward curvature at the boundaries specifically at pH levels above 10.2 combined with extreme reagent dosages suggests a loss of selectivity. This behaviour reinforces that while pH is a secondary factor compared to dosage, its control is vital to avoid regions of marginal inadequacy where silica levels exceed the 0.50% threshold.

The interaction effects on metal recovery (R_m) are illustrated in the response surfaces and contour plots of Figure 6. As shown in Figure 6(a), there is a synergistic relationship between starch and amine dosages; increasing the starch dosage consistently promotes higher recovery, with values exceeding 90% in the region of high starch concentration. Conversely, the lowest recovery levels (below 80%) were observed when low starch dosages (<340 g/t) were combined with high amine concentrations (160–240 g/t), a condition that favours the unintended flotation of iron oxides due to insufficient depression. The interaction between pH and starch (Figure 6(b)) demonstrates that starch effectively enhances R_m across the entire tested pH range. A critical threshold is observed near 360 g/t of starch; below this level, R_m drops significantly to less than 75%, regardless of the pH, highlighting the indispensable role of the depressant. Furthermore, the interaction between pH and amine (Figure 6(c)) reveals that at pH levels below 10.20, high amine dosages (>175 g/t) lead to a substantial reduction in recovery. However, for amine dosages below 175 g/t, high recovery is maintained independently of the pH level. These results confirm that while the system is robust, the balance between collector and depressant dosages is the primary factor in maximising metal recovery while maintaining concentrate quality.

5.5. Optimisation of the metal recovery response

To identify the optimal operating conditions for the variables evaluated in this study, the Generalised Reduced Gradient (GRG) algorithm was employed. The optimisation objective was to maximise metallic recovery (R_m) while maintaining the concentrate quality within industrial specifications. This process utilised

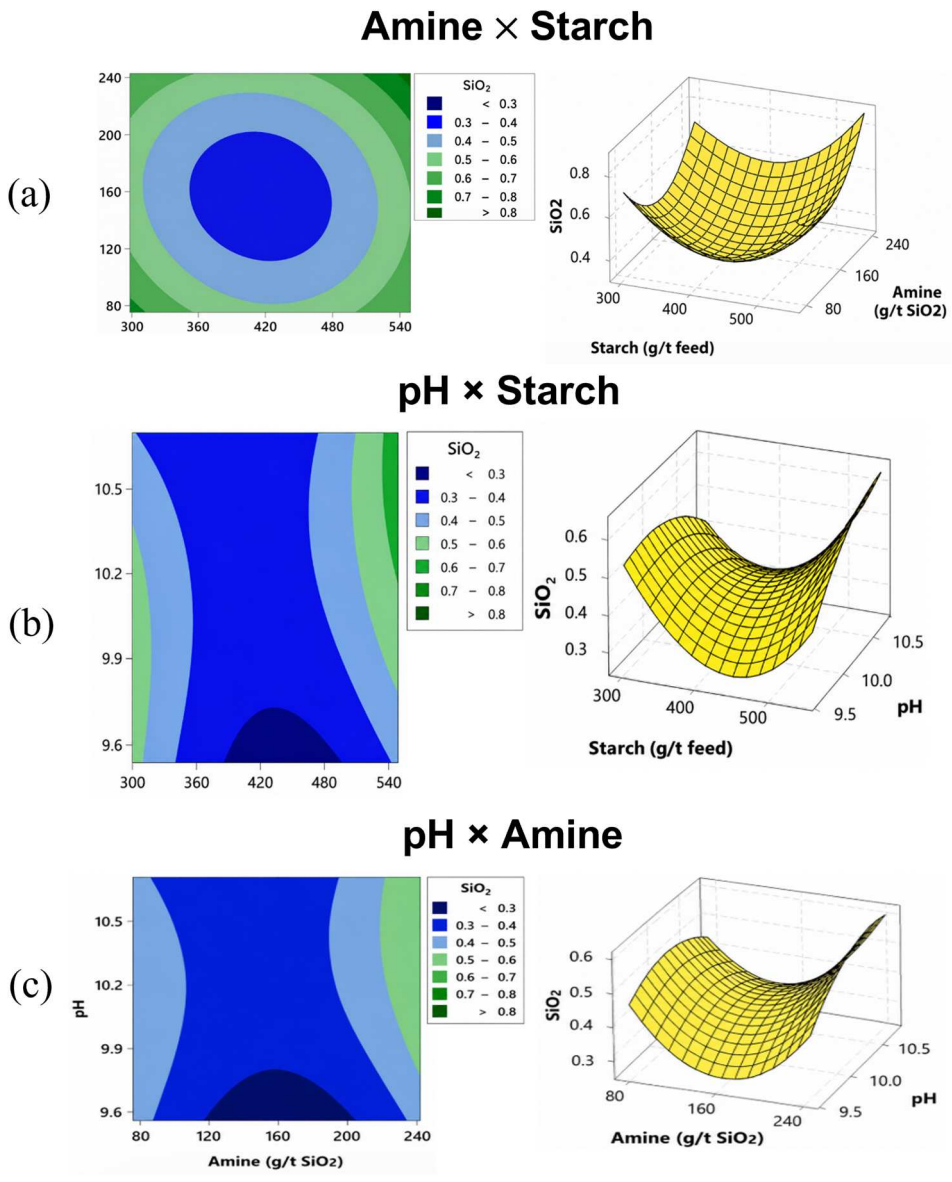

Figure 5. Response surface and contour plots for SiO_2 content: (a) amine and starch interaction; (b) pH and starch interaction; (c) pH and amine interaction.

response data from the rougher/cleaner and scavenger flotation stages, as defined by the Central Composite Design (CCD). Following the ANOVA, the regression models were refined, and only the coefficients associated with statistically significant terms ($p < 0.05$) were retained. These significant regression coefficients for each response variable (Fe, SiO_2, P, Al_2O_3, Mn, and PPC) are summarised in Table 7. From an analytical standpoint, the nonlinear optimisation problem aimed at maximising R_m is governed by the objective function presented in Equation (9).

From an analytical standpoint, the nonlinear optimisation problem aimed at maximising metal recovery (R_m) is expressed by the objective function presented in Equation (9).

$$\begin{aligned} &\text{Maximize} && R_m \\ &\text{Subject to:} && \%\ SiO_2 \leq 0.50\% \\ & && 67.50\% \leq \%Fe \leq 69.50\% \\ & && 350 \leq \text{starch}(g/t_{feed}) \leq 500 \\ & && 75 \leq \text{amine}(g/t_{SiO_2}) \leq 200 \\ & && 9.80 \leq \text{pH} \leq 10.50 \end{aligned} \tag{9}$$

5.6. Global optimization and model validation

The data were compiled into a specialised spreadsheet where the GRG (Generalised Reduced Gradient) algorithm was executed using the Microsoft Excel® Solver

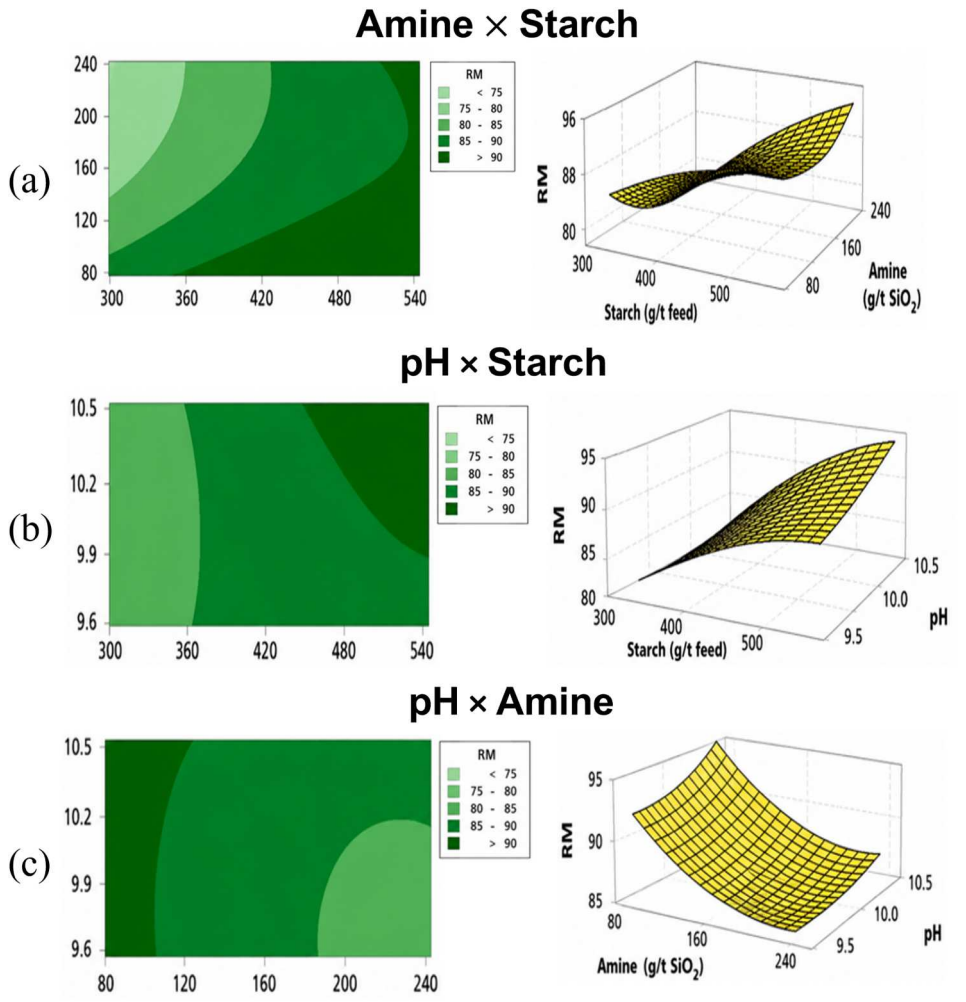

Figure 6. Response surface and contour plots for metal recovery (R_m): (a) amine and starch interaction; (b) pH and starch interaction; (c) pH and amine interaction.

tool to determine the optimal operating conditions. The nonlinear constraint function was solved to maximise metallic recovery (R_m), yielding an optimal configuration of 500 *g*/*t* of starch, 75 *g*/*t* of amine, and a pH of 9.80.

Applying this optimised solution to the predictive models for each mineral resulted in a calculated pellet feed composition with a metallic recovery of 95.21%, as presented in Table 8. The concentrate achieved high chemical quality, notably with SiO_2 levels at 0.46% and Iron (*Fe*) content at 69.08%, meeting the strict requirements for high-grade pelletising feed. To ensure the reliability of these findings, a confirmation experiment was conducted using the parameters defined by the optimised solution. This validation test allowed for a direct comparison between the experimental results and the values predicted by the GRG-optimised model, as summarised in Table 9.

Table 7. Significant regression coefficients of the responses.

	Fe	SiO_2	*P*	Al_2O_3	Mn	PPC
b_0	69.08	0.3491	0.0126	0.101	0.02767	0.30
b_1	0.00	0.0000	0.0000	0.000	−0.00118	0.00
b_2	0.00	0.0000	0.0007	0.000	0.00000	0.00
b_3	0.00	0.0000	0.0000	0.000	0.00184	0.00
b_{11}	0.00	0.0000	0.0009	0.000	0.00136	0.00
b_{22}	0.00	0.1068	0.0000	0.000	0.00000	0.00
b_{33}	0.00	0.0000	0.0000	0.000	0.00000	0.00
b_{12}	0.00	0.0000	0.0000	0.000	0.00000	0.00
b_{13}	0.00	0.0000	0.0000	0.000	0.00000	0.00
b_{23}	0.00	0.0000	0.0000	0.000	0.00000	0.00

Table 8. Mineral content of pellet feed calculated using the optimal model solution.

Flow	Fe	SiO_2	*P*	Al_2O_3	Mn	PPC	R_m
Feed	49.24	28.36	0.016	0.33	0.022	0.38	**95.21**
Pellet feed	69.08	**0.46**	0.013	0.10	0.026	0.30	

Table 9. Summary of the confirmatory test results.

Flow	*Fe*	SiO_2	Metal recovery (%)	Mass recovery (%)
Feed	49.24	28.36		
Concentrate	68.89	0.51	93.86	67.09
Tailing	9.19	85.19		

5.7. Model validation through confirmatory experiment

To validate the mathematical model's accuracy, a confirmation experiment was conducted using the optimised parameters (500 g/t starch, 75 g/t amine, and pH 9.80). The experimental results, summarised in Table 9, show that the metallic recovery (R_m) reached 93.86%. This value is remarkably close to the model's theoretical prediction of 95.21%, with a minor deviation of only 1.35%. Furthermore, the concentrate obtained in this test surpassed the performance of 15 out of the 16 experimental runs from the initial design. Although the SiO_2 content (0.51%) was marginally above the 0.50% threshold, it is significantly better than the results from Run 6, which was the only individual test to yield a higher recovery but with non-compliant silica levels. This close agreement between experimental and predicted data demonstrates the robustness and reliability of the quadratic models developed in this study for predicting the behaviour of complex mineral samples.

The metallic recovery obtained in the confirmation experiment was 93.86%, which exceeded the results of 15 out of the 16 experimental conditions evaluated in this study. Considering the maximum allowable SiO_2 content of 0.50% in the concentrate, the optimised condition provided a higher R_m than all other experimental configurations that met the quality standards. The observed recovery of 93.86% was approximately 1.35% lower than the theoretical value predicted by the model (95.21%), demonstrating a strong agreement between the experimental and expected results. It is worth noting that while Run 6 yielded a higher recovery than the optimised test, it also exhibited a SiO_2 content exceeding the specified 0.50% limit. Such non-compliance would incur significant penalties in the product's market value, confirming that the optimised solution (*GRG*) successfully identified the best balance between high metallurgical performance and strict chemical specifications.

6. Conclusion

From the perspective of optimising flotation parameters to maximise metallic recovery while maintaining SiO_2 content within quality limits, satisfactory results were achieved using a Central Composite Design (CCD) combined with the Generalised Reduced Gradient (GRG) algorithm. The optimal condition was identified at 500 g/t of starch, 75 g/t of amine, and pH 9.80. This was validated experimentally, yielding a metallic recovery (R_m) of 93.86% with 0.51% SiO_2 in the concentrate.

The statistical modelling provided determination coefficients R^2adj of 0.9478 for R_m and 0.2429 for SiO_2 content. While the recovery model showed high statistical significance ($p < 0.001$), the SiO_2 model demonstrated that the response is less sensitive to the studied ranges ($p = 0.310\$$), although it effectively guided the identification of the optimal region. The process performance was favoured by the high proportion of free quartz identified in the mineralogical analysis and a favourable particle size distribution (0.150 mm to 0.045 mm) with minimal ultrafine interference.

The analysis of main and interaction effects revealed that:

- pH had the least influence on the responses, indicating a robust operational window.
- Starch and Amine dosages were the most influential parameters, with the collector (amine) showing the strongest impact on R_m reduction when in excess, due to the entrainment of iron-bearing particles.
- Optimisation balance: Lower SiO_2 contents were obtained through intermediate dosages of starch and amine at lower pH values, while higher R_m was consistently achieved using high starch and low amine dosages.

In general, this study demonstrates the feasibility of modelling flotation responses through Response Surface Methodology (RSM) and the GRG algorithm. This approach represents a relevant contribution, aligning with industrial needs for rapid and economic experimental optimisation. The results obtained reflect practical industrial conditions, and the optimised ranges identified can serve as reference limits for advanced process control. Given the inherent variability of Run-of-Mine (ROM) feed, periodic experimental reassessments are recommended to ensure these control limits remain effective.

Acknowledgement

The authors would like to gratefully acknowledge the National Council for Scientific and Technological Development (CNPq), the Coordination for the Improvement of Higher Education Personnel (CAPES), the Minas Gerais State Agency for Research and Development (FAPEMIG), the Mining Company Vale S.A., and GEQProd for their support in this research.

Disclosure statement

No potential conflict of interest was reported by the author(s).

ORCID

Tarcísio Gonçalves de Brito http://orcid.org/0000-0001-6364-2359

References

[1] Zhang X, Gu X, Han Y, et al. Flotation of iron ores: a review. Miner Process Extr Metall Rev. 2021;42:184–212. doi:10.1080/08827508.2019.1689494

[2] Box GE, Draper NR. Response surfaces, mixtures, and ridge analyses. 2nd ed. Hoboken (NJ): John Wiley & Sons. 2007.

[3] Matos VE, Nogueira SC, Silva GR, et al. Effects of surfactants combination on iron ore flotation. Miner Eng. 2022;190:107910. doi:10.1016/j.mineng.2022.107910

[4] Lima NP, Valadão GES, Peres AEC. Effect of amine and starch dosages on the reverse cationic flotation of an iron ore. Miner Eng. 2013;45:180–184. doi:10.1016/j.mineng.2013.03.001

[5] Filippov LO, Severov VV, Filippova IV. An overview of the beneficiation of iron ores via reverse cationic flotation. Int J Miner Process. 2014;127:62–69. doi:10.1016/j.minpro.2014.01.002

[6] Vieira AM, Peres AEC. The effect of amine type, pH, and size range in the flotation of quartz. Miner Eng. 2007;20:1008–1013. doi:10.1016/j.mineng.2007.03.013

[7] Lima RMF, Brandao PRG, Peres AEC. The infrared spectra of amine collectors used in the flotation of iron ores. Miner Eng. 2005;18:267–273. doi:10.1016/j.mineng.2004.10.016

[8] Kumar R, Mandre NR. Development of a statistical model for selective flocculation of iron ore slimes. J Dispers Sci Technol. 2016;37:231–238. doi:10.1080/01932691.2015.1039024

[9] Pattanaik A, Rayasam V. Analysis of reverse cationic iron ore fines flotation using RSM-D-optimal design – an approach towards sustainability. Adv Powder Technol. 2018;29:3404–3414. doi:10.1016/j.apt.2018.09.021

[10] Rath SS, Sahoo H, Das B. Optimization of flotation variables for the recovery of hematite particles from BHQ ore. Int J Miner Metall Mater. 2013;20:605–611. doi:10.1007/s12613-013-0773-9

[11] Montgomery DC. Design and analysis of experiments. 8th ed. Hoboken (NJ): John Wiley & Sons, Inc.; 2013.

[12] Chen M, Fan SS. Tolerance evaluation of minimum zone straightness using non-linear programming techniques: a spreadsheet approach. Comput Ind Eng. 2002;43:437–453. doi:10.1016/S0360-8352(02)00057-8

[13] Paiva AP, Ferreira JR, Balestrassi PP. A multivariate hybrid approach applied to AISI 52100 hardened steel turning optimization. J Mater Process Technol. 2007;189:26–35. doi:10.1016/j.jmatprotec.2006.12.047

[14] Acosta-Flores R, Lucay FA, Cisternas LA, et al. Two-phase optimization methodology for the design of mineral flotation plants, including multispecies and bank or cell models. Miner Metall Process. 2018;35:24–34. doi:10.19150/mmp.8055

[15] Turan MD. Statistical approach to mineral engineering and optimization, in contributions to mineralization. In Tech. 2018;71607. doi:10.5772/intechopen.71607

[16] Vesa I, Sppragon M, Fattah IMR, et al. Response surface methodology (RSM) for optimizing engine performance and emissions fueled with biofuel: review of RSM for sustainability energy transition. Results in Engineering. 2023;18:101213. doi:10.1016/j.rineng.2023.101213

[17] Scott JL, Smith RW. Diamine flotation of quartz. Miner Eng. 1991;4:141–150. doi:10.1016/0892-6875(91)90030-Y

[18] Jankovic A, Chaudhary G, Goia F. Designing the design of experiments (DOE) – an investigation on the influence of different factorial designs on the characterization of complex systems. Energy Build. 2021;250:111298. doi:10.1016/j.enbuild.2021.111298

[19] Köksoy O, Doganaksoy N. Joint optimization of mean and standard deviation using response surface methods. J Qual Technol. 2003;35:239–252. doi:10.1080/00224065.2003.11980218

[20] Köksoy O. A nonlinear programming solution to robust multi-response quality problem. Appl Math Comput. 2008;196:603–612. doi:10.1016/j.amc.2007.06.023

[21] Luenberger DG. Linear and nonlinear programming. 2nd ed. Rading (MA): Addison-Wesley; 1989.

[22] Lasdon LS, Waren AD, Jain A, et al. Design and testing of a generalized reduced gradient code for nonlinear programming. ACM Trans Math Softw. 1978;4:34–50. doi:10.1145/355769.355773

[23] Araújo AC, Amarante SC, Souza CC, et al. Ore mineralogy and its relevance for selection of concentration methods in processing of Brazilian iron ores. Miner Process Extr Metall. 2003;112:54–64. doi:10.1179/037195503225011439

[24] Lima NP, Pinto TCS, Tavares AC, et al. The entrainment effect on the performance of iron ore reverse flotation. Miner Eng. 2016;96-97:53–58. doi:10.1016/j.mineng.2016.05.018

[25] Karimifard S, Moghaddam MRA. Application of response surface methodology in physicochemical removal of dyes from wastewater: a critical review. Sci Total Environ. 2018;640-641:772–797. doi:10.1016/j.scitotenv.2018.05.355